OPTIMIZETION OF ACTUATING SYSTEM FOR FLAPPING ROBOT DESIGN

T. Imura[a], M. Fuchiwaki[b], K. Tanaka[b]

[a] *Graduate School of Computer Science and Systems Engineering Kyushu Institute of Technology*
680-4 Kawazu, Iizuka-cit, Fukuoka 820-8502, Japan
Research Fellow of the Japan Society for the Promotion of Science
[b] *Department of Mechanical Information Science and Technology Kyushu Institute of Technology*
680-4 Kawazu, Iizuka-city, Fukuoka 820-8502, Japan

[a]imura@vortex.mse.kyutech.ac.jp , [b]futiwaki@mse.kyutech.ac.jp , [c]kazuhiro@mse.kyutech.ac.jp

ABSTRACT

In this paper, my purpose is suggestion for design method for actuating system of flapping robot. It is necessary to develop that. Considering the drag of flapping wings and the characteristic of motor revolution for its load, the actuating system of flapping robot is modeled. The motor whose resultant flapping frequency and wing loading required for flapping robot is selected, and flapping robot is developed by that result. As the result, the flapping robot can fly stably for about 15 minutes. Moreover, the design method is effective in case of attaching important to the increase in flight altitude by clarifying that flapping frequency play an important role for control of flight altitude.

Keywords: flapping robot design, tailless airplane, actuating system modeling, optimizing actuating system

1. INTRODUCTION

1990s, Defense Advanced Research Projects Agency (DARPA) led developing small airplane called Micro air vehicles (MAVs) with a maximum dimension of 15 [cm] or less and a flight speed of 10 [m/s]. MAVs are expected to both military and civilian applications, especially surveillance and reconnaissance at a remote or otherwise hazardous location and at the other planets. As rapid advance in power source miniaturization, structures, materials, control device and communication technology, many researchers have developed many MAVs of fixed wing, rotation wing and flapping wing (Yongsheng L., Wei Shyy, D. Viieru and B. Zhang 2003; Robert C. Michelson 2008; Zaeem A .Khan and Sunil K. Agrawal 2006).

As the result of evolution of life for several 100 millions of years, insects, birds and bats are recognized as the most effective flying object. In nature flying objects, the flight systems such as wing structure, wing kinematics, and flight controlling are optimized and harmonized well. It has been clarified that insects and birds fly with many mechanism, i.e. delayed stall, rotational circulation, wake capture, clap and fling and so on (F. O. Lehmann 2004; M.H.Dickinson, F.O.Lehman, S.P.Sane 1999; T.Maxworthy 1979). Many researchers have taken notice and reported for the force generation mechanism on the flights of insects and birds and so on.

In many kinds of insect which is taken notice by them, it is well known that a butterfly combines flapping wing motion with gliding and the figure of flying is very beautiful. Moreover, butterflies do not perform linearly flying motions similar to dragonfly, but they perform motion like dancing with low flapping frequency. Sunada et al. observed Pieris melete on a taking-off flight and reported on characteristics of behaviors of a butterfly wings, its center of gravity and its abdomen and so on (S. Sunada, K. Kawachi, I. Watanabe, and A. Azuma 1993).

The concept called Biomimetics by which nature creatures is mimicked has been taken notice. Based on this concept, a lot of flapping robots to which the insect and bird flight mechanisms, i.e. Flapping resonance, Traverse bending, Clap and fling and so on, were applied have reported (Robert J. Wood 2008; Zaeem A .Khan and Sunil K. Agrawal 2006; De Croon G.C.H.E., de Clerq K.M.E., Ruijsink R., Remes B., and de Wagter C. 2009). However, almost of that have taken notice on whether robot can fly or not, and unsteady aerodynamic forces generated by wing flapping. From the result, it is the present situation that the reports which take notice on design and developing method of flapping robot are a few.

In this paper, my purpose is suggestion for method of optimization for actuating system of flapping robot. It is necessary to develop that. Concretely speaking, considering the drag of flapping wings and the characteristic of motor revolution for its load, optimized motor and reduction ratio of actuating system for flapping robot is selected. Moreover, flapping robot is developed by that result, and its flight is evaluated by flight observation experiment.

2. MODELIZATION OF FLAPPING SYSTEM
2.1. Modeling of actuating system and wings

In this chapter, the actuating system of flapping robot is modeled due to estimate flapping frequency from motor specification. Fig. 1 shows a pattern diagram of actuating system for flapping. Flapping motion is powered by an electric motor through a

gearbox to reduce rotational speed and load at motor. A crank rotation conducted from a gearbox is transformed to linear motion with linkage mechanism. The linear motion actuates the wings which are made of thin Japanese paper and light carbon rods, and flapping robot performs flapping motion. This flapping robot operates flapping motion as wing deforms because the wing membrane is consist of Japanese paper. However it is expected that each value of wing changes by flapping because of wing tenderness, the author models with 1 period averages, not considering dynamic effects, due to design actuating system.

The revolution of motor ω_M [Hz] changes lineally for the load of motor. Therefore, ω_M is shown by Eq. 1. In the Eq. 1, k_t [Hz/(N*m)], N [Hz] and T [N*m] show the gradient of revolution for load at motor, revolution at no load and torque (load) at motor, respectively. In this way, a motor part of actuating system is modeled.

$$\omega_M = N - k_t T \qquad (1)$$

The load (torque) generated at motor is shown simply by Eq. 2. In the Eq. 2, T_ω [N*m] and T_o [N*m] show load (near to drag) by wing flapping and load by such as friction except the load by flapping motion at whole system, respectively. G shows reduction ratio, and T [N*m] inversely relates to G.

$$T = \frac{T_\omega + T_0}{G} \qquad (2)$$

Considering the inverse relation between ω_M and G, the revolution of gear connected to the wings through linkages (equal to flapping frequency) ω is shown by Eq.3 which is obtained from Eq.1 and 2. Eq.3 is function which shows relation between reduction ratio, torque, motor characteristics and flapping frequency, respectively. In this way, motor and gearbox parts of actuating system are modeled. Then, main motor load by wing drag generated with flapping motion is conducted.

$$\omega = \frac{NG - k_t(T_\omega + T_0)}{G^2} \qquad (3)$$

Fig.2 shows a pattern diagram for calculating wing drag. The wing velocity changes for the position on the wing span direction, because the wings perform flapping motion which is similar to rotating. In this paper, the wing velocity is approximated to $r\omega$, simply. a [m], b [m] and r [m] show wing span length, wing chord length and position for wing span direction, respectively. The partial torque (load) fom r of wing position dT_ω [N*m] shows multiplication of partial drag at r of position dD [N] and r [m] (Eq.4). The partial torque generated at basis of wing $dT\omega$ from the partial area of wing dS is shown by Eq.5. In the Eq.5, C_D, ρ and U show drag coefficient of wing, density, flapping velocity at dS.
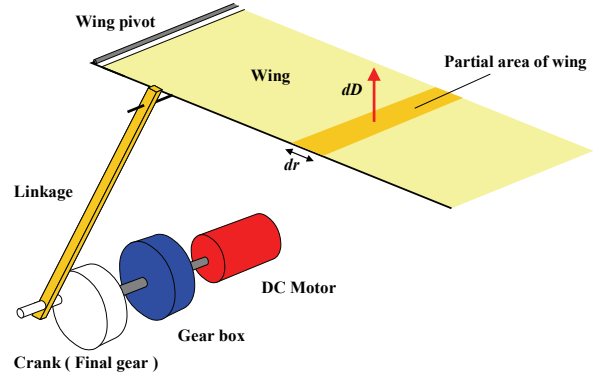

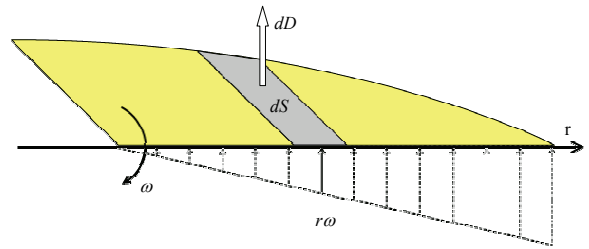Figure 1: Pattern Diagram of Flapping Actuating System
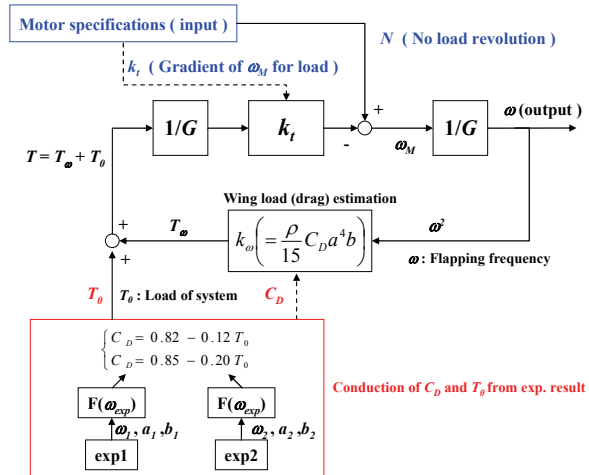

Figure 2: Pattern Diagram for Calculating Wing Drag

Figure 3: Model for Estimating Flapping Frequency

$$dT_W = rdD \qquad (4)$$

$$dT_W = r\frac{\rho}{2}C_D U_{(r)}^2 dS \qquad (5)$$

Considering two factors which are wing shape is a quarter of ellipse and U shows $r\omega$, the load (torque) from wings is shown by Eq.6.

$$T_\omega = \int_0^a r\frac{\rho}{2}C_D(r\omega)^2 b\sqrt{1 - \frac{r^2}{a^2}}dr$$
$$= \frac{1}{15}\rho C_D a^4 b\omega^2 \qquad (6)$$

302

Flapping frequency ω is shown by Eq.7 from Eq.3 and 6. In this way, the model of actuating system considering the load at motor by wing drag with flapping is constructed.

This model is assumed that drag coefficient which is affect by wing deformation is constant because this model is recommended for using and calculation 1 period average. Moreover, this model is assumed that wings have uniform motion at mean velocity although actual wing velocity always oscillates. As the result, dynamic oscillation of wing deformation and wing velocity is not modeled in this model. On the other word, this model is nearly equal to a static model which motor revolution is conduct from torque which generates on the fixed rigid airfoil in different flow velocity distribution at wing tip and base of wing. For this reason, this model is not suitable for calculating dynamic values as wing flaps. Therefore, 1 period average is applied for estimating flapping frequency in this model.

Moreover, in this model, it seems to consider that the error between estimating value and real one when flapping frequency is very different from measuring value due to not model wing deformation as it changes by flapping frequency.

$$\omega = \frac{-G^2 + \sqrt{G^4 + 8k_T k_\omega NG + 8k_T^2 k_\omega T_0}}{4k_T k_\omega} \quad (7)$$

$$k_w = \frac{\rho}{15} C_D a^4 b$$

Fig.3 shows a block diagram of this model. The input of this model is no load revolution N [Hz] and gradient of revolution for load at motor k_t [Hz/(N*m)], and the output is flapping frequency ω [Hz]. Therefore, it is possible that a suitable motor is selected for flapping robot by estimating flapping frequencies for each motor.

However flapping frequency can be estimated with inputting motor specifications (k_t [Hz/(N*m)] and N [Hz]), load at motor T [N*m] and reduction ratio G, the wing load with flapping is proportional to the square of flapping frequency ω^2. As the result, this block diagram has closed-loop. Because it is difficult to conduct the wing drag coefficient C_D and load except the load by flapping motion at whole system T_0, they are conducted by experimental results. In the chapter 2.2, C_D and T_0 are conducted from the result of experiment and Eq.7.

2.2. Derivation of coefficient value

In this chapter, the wing drag coefficient C_D and load at whole system T_0 are conducted by Eq.7 and experiment of measuring flapping frequency. Fig.4 shows the experimental apparatus for flapping frequency measuring. This apparatus consists of flapping robot and high speed camera (1125[fps]). The flapping frequency of flapping robot fixed on a shaft is measured with image measurement. In concrete terms,
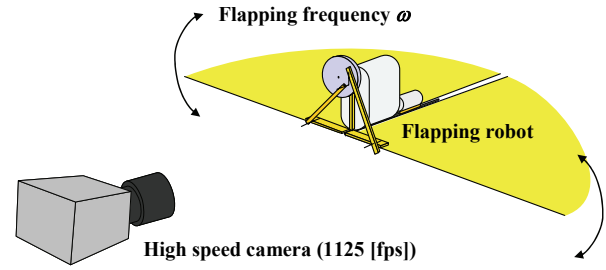

Figure 4: Experimental Apparatus for Measuring Flapping Frequencies

the time span for 10 periods flapping is measured with high speed camera, and the time span required for 1period flapping is calculated from measuring value. Flapping frequency is equal to the reciprocal of this calculating value. The wing drag coefficient is calculated with back calculation from the flapping frequency. Eq.8 shows a function for back calculation and is conducted from Eq.7. Because the wing drag coefficient C_D with back calculation contains the load at whole system T_0 (Eq.9), the wing drag coefficient C_D and load at whole system T_0 are conducted by measuring flapping frequencies of 2 kinds of wing which have different wing area. In this calculation, the author assumes that the wing drag coefficient C_D is constant for wing area and deformation and load at whole system T_0 is constant for flapping frequency.

$$C_D = \frac{NG - \omega G^2 - k_t T_0}{2k_{\omega 2} k_t \omega^2} \quad (8)$$

$$k_{\omega 2} = \frac{\rho}{15} a^4 b$$

When a wing areas are 8.2 *10^{-3} [m^2] and 6.5 *10^{-3} [m^2], flapping frequencies are 7.51 [Hz] and 10.04 [Hz], respectively. The drag coefficient C_D of wings which have different wing area and flapping frequency is calculated by Eq.8 and flapping frequencies(Eq.9). As previously described, because the wing drag coefficient C_D with back calculation contains the load at whole system T_0 in mathematical expression which can calculate drag coefficient from flapping frequency with back calculation, the wing drag coefficient $C_D = 0.690$ and load at whole system $T_0 = 0.192$ [N*m] is conducted by two equations of Eq.9. The calculated wing drag coefficient C_D is smaller than drag coefficient C_D = about 2.3 (angle of attack of 90 [deg.]) which is estimated by steady aerodynamic force at the rigid wing mimicking wing shape of a kind of hawk moth (F. O. Lehmann 2004). In addition to different wing shape and experimental method between this study and hawk moth result, the wings deform largely with flapping motion because the wing membrane is Japanese paper in this study and its arc parts of wing are free end condition. It seems to consider that the drag coefficients C_D of this study is smaller than that of rigid

wing because of decrease in projected area of wing against wing motion direction by wing deformation.

When flapping frequency is different extremely from that of experimental result, it is expected that actual wing deformation value changes largely from value on the assumption. Not surprisingly, it is expected that the actual drag coefficients C_D is different from that of this study because of assumption which drag coefficient C_D is constant for wing deformation in this model. As the result, it seems that the error of estimated flapping frequency increases. From this result, it is not suitable for estimating flapping frequency for extremely different frequency from around flapping frequency of 10 [Hz].

In chapter 3, the optimized motor and reduction ratio is selected by C_D, T_0 conducted in this chapter and Eq.7, and the actuating system is designed.

$$\begin{cases} C_D = 0.82 - 0.12T_0 \\ C_D = 0.85 - 0.20T_0 \end{cases} \quad (9)$$

3. DESIGN OF ACTUATING SYSTEM FOR FLAPPING ROBOT

3.1. Required values for flapping robot

In this study, flapping robot applied by butterfly flight is suggested and developed it. Fig.5 shows the relation between wing loading, flapping frequency and wing aspect ratio of Lepidoptera (mainly butterflies and moths) from literatures of butterfly. The horizontal axis shows wing loading, and the left and right vertical axes show flapping frequency and aspect ratio of wing, respectively. The red circles and black circles show that of butterflies and that of moths, respectively. The soild circles and the midair circles show flapping frequency and aspect ratio of wing, respectively. The flapping frequency, wing loading and aspect ratio of butterfly are approximately 7 - 15 [Hz], 0.5 - 1.5 [N/m^2] and 1.5 – 3.0. Especially, it is well known that flapping frequency directly affects unsteady aerodynamic forces by wing flapping (Che-Shu Lin, Chyanbin Hwu and Wen-Bin Young 2006), and it is clear from Eq.6 which is used for modelization in this paper. In this paper, the author intends to make flapping frequency and wing loading of flapping robot to approximate to these data.

H. Tanaka et al. clarified that an appropriate position of the center of gravity makes the balance of longitudinal moment, and it leads to stable forward flight. In his experiment, when center of gravity was at $0.34C$ against wing chord length C [m], stable forward flight was realized (H. Tanaka, K. Hoshino, K. Matsumoto, and I. Shimoyama 2005). The flapping robot in this study has also similar position of center of gravity, and its position is $0.33C$.

3.2. Optimization of motor for actuating system of flapping robot

Fig.6 shows flapping frequencies and wing loadings of each motor. The horizontal and vertical axes show

flapping frequency and wing loading, respectively. The wing loading is estimated from total
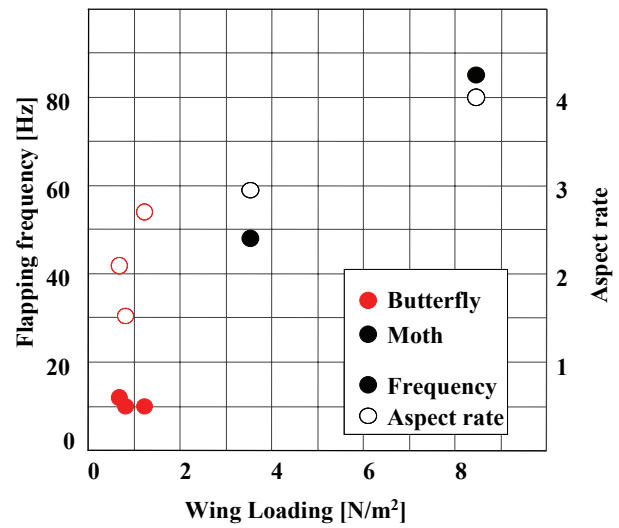

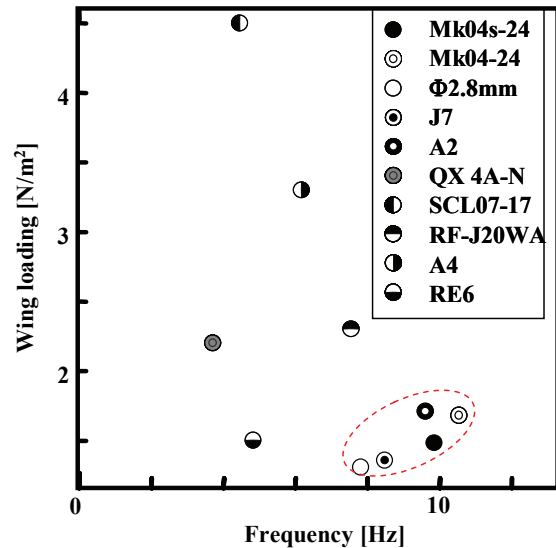Figure 5: Specification of butterflies and Moths

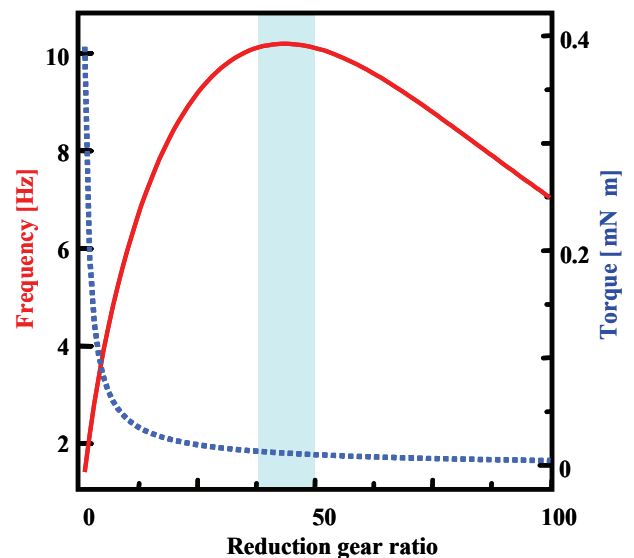Figure 6: Optimized Motors for Actuating System

Figure 7: Optimized Reduction Ratio for Actuating System weight which is conducted by adding 1.5 [g] to motor weight, and aspect ratio, drag coefficient and reduction ratio are 3.0, 0.775 and 40.0, respectively.

As previously described, flapping frequency of 7-15 [Hz] and wing loading 0.5-1.5 [N/m2] are required to flapping robot. Therefore, the motors near red circle (Mk04s-24, Mk04-24, A2, ϕ 2.8mm and J7) are suitable for motor of actuating system. In this paper, Mk04-24 is used for flapping robot, because it is expected that flapping frequency which affect unsteady aerodynamic forces is important for flight. Not surprisingly, this judgmental standard can change by intention of developer. For instance, J7 is the optimized motor if the developer requires a light weight flapping robot.

3.3. Optimization of reduction ratio for actuating system of flapping robot

The reduction ratio of actuating system affects flapping frequency as it is clear from Eq.7. Therefore, it seems to consider that estimating optimized reduction ratio is important factor for developing flapping robot. In this chapter, the optimized reduction ratio is estimated for obtaining high flapping frequency with conducted model.

Fig.7 shows the relation between reeducation ratio and flapping frequency. The horizontal and vertical axes show reduction ratio and flapping frequency respectively. The solid and dashed lines show flapping frequency and load (torque) at motor. The selected motor, aspect ratio, drag coefficient and wing loading are Mk04-24, 3.0, 0.775 and 1.4 [N/m^2], respectively. The flapping frequency increases as reduction ratio enlarges, and it becomes peak at reduction ratio of 40-50. When reduction ratio is larger than 50, the flapping frequency decreases. Because actual reduction ratio depends on combination of gears, it is distributed discretely. The numbers of light, small and commercial gear teeth are 9, 12, 40, 60 and 90, considering these combinations, reduction ratio of 44.4 (Using 4 gears; the no. of teeth are 9, 9, 60, 60) can be realized. As the result, the reduction ratio of 44.4 is used for flapping robot in this paper.

4. FLAPPING ROBOT AND ITS FLIGHT

Fig.8 and Table 1 show a developed flapping robot and its specification. The developed flapping robot does not have tail plane as Fig.8 shows. Its wing span length, chord length and weight are 40 [mm], 80 [mm] and 1.97 [g], respectively, and the author achieves developing for small and light flapping robot. This flapping robot can fly with range of flapping frequency of 7 – 11 [Hz] by adjusting the voltage which battery applies to. The flapping frequency is higher than estimating flapping frequency of approximately 10 [Hz] because the flapping frequency on free flight tends to be higher than that on fixed flight. It has already been confirmed that the flapping frequency on fixed flight is approximately 10 [Hz].

Figure 8: Flapping Robot without Tail Plane

Table 1: Specifications of Flapping Robot

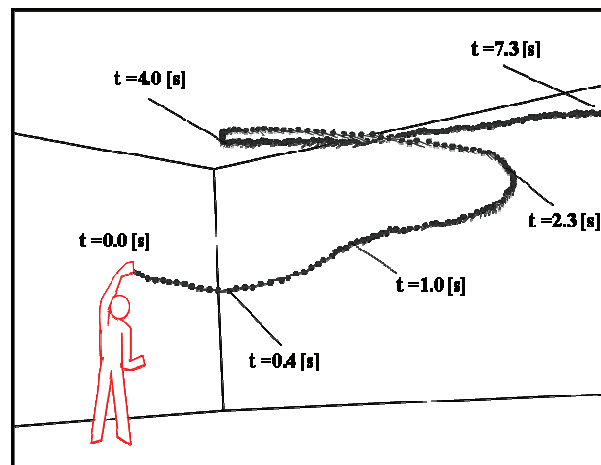| Wing span length	240	[mm]
Wing chord length	80	[mm]
Mass	1.9	[g]
Wing loading	1.5	[W/m^2]
Flapping frequency	7 ~ 11	[Hz]
Aspect ratio	3.0	
battery endurance	15	[min]

Figure 9: Flight Trajectory of Flapping Robot

In this flapping robot, the mean pitch angle, vertical flight velocity and yaw angle can be adjusted by dihedral angle of wing, flapping frequency and mounting position of both wings. The flight can be controlled by adjusting these parameters. However these adjust is static, the flight can be controlled in case of dynamic change of flapping frequency and mounting position. Therefore, the flight altitude and direction can be commanded remotely by remote control of these parameter. On the other words, the flight of this flapping robot can be controlled remotely.

Fig.9 shows flight trajectory of flapping robot. The symbol *t* in this figure shows elapsed time from flight starting. Between flight time t = 0.0 [s] and t = 1.0 [s], the flight altitude once vibrates. After t = 1.0 [s], flapping robot continues to increase the flight altitude stably. At the around t = 2.3 [s], flapping robot begins to turn right. Between t = 2.3 [s] and t = 4.0 [s] approximately, flapping robot change turning direction from toward right to toward left. At the around t = 4.0 [s], flapping robot turns left and flies stably. After t = 7.3 [s], flapping robot goes out range of camera. Until t = 7.3 [s], the flight altitude continues to increase despite of flight direction variation. From this result, developed flapping robot can fly upward with flight direction variation except flight starting 1 second, and it can fly for about 15 minutes.

Fig.10 shows the vertical velocity of flapping robot on the stable flight with different flapping frequencies. The horizontal and vertical axes show flapping frequency and vertical flight velocity. The red circles and the blue circles indicate flight which vertical velocity is lower than 0 [m/s] and higher than 0 [m/s], respectively. The red line indicates straight line of linear approximation. It is understood that vertical velocity increases linearly from -0.3 [m/s] to 0.3 [m/s] between flapping frequency of 7.8 [Hz] and 10.5 [Hz], and the gradient of that is 0.20 [m/s*Hz]. From this result, flapping frequency affects for vertical flight velocity, and it is confirmed that flapping frequency is important parameter for control of flight altitude. Moreover, from these results, it seems to consider that designing method which can select optimized motor and reduction ratio by estimating flapping frequency which is important parameter for control of flight altitude with modeling of wings and actuating system is effective for flapping robot developing.

5. CONCLUDING REMARKS

Considering wing drag and characteristics of motor, actuating system of flapping robot is modeled, and the designing method with its model for actuating system is suggested. With its designing method, actuating system is designed, and small and light flapping robot which can fly for about 15 minutes is developed. Moreover, from these results, it seems to consider that designing method which can select optimized motor and reduction ratio by estimating flapping frequency which is important parameter for control of flight altitude with modeling of wings and actuating system is effective for flapping robot developing.

REFERENCES

Yongsheng L., Wei Shyy, D. Viieru and B. Zhang, 2003. Membrane wing aerodynamics for micro air vehicles, *Progress in Aerospace Sciences*, 39, pp. 425–465

Robert C. Michelson, 2008. Test and Evaluation of Fully Autonomous Micro Air Vehicles, *The ITEA Journal*, 29(4), pp. 2-11
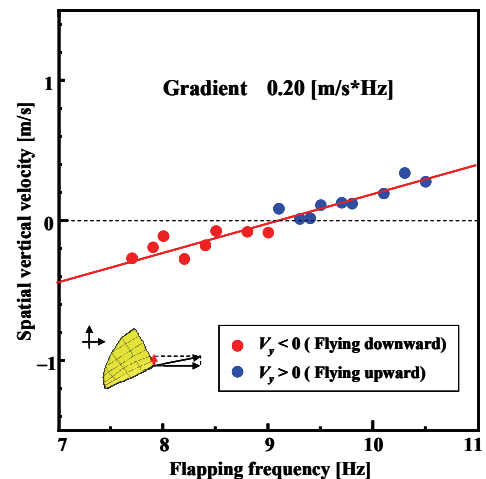
Figure 10: Relation between Flapping Frequency and Vertical Velocity

Zaeem A .Khan and Sunil K. Agrawal, 2006. Design of Flapping Mechanisms Based on TransverseBending Phenomena in Insects, *IEEE International Conference on Robotics and Automation*, pp. 2323-2328, May 2006, Orlando, Florida

F. O. Lehmann, 2004. The mechanisms of lift enhancement in insect flight, *Naturwissenschaften*, 91, pp. 101-122

M.H.Dickinson, F.O.Lehman, S.P.Sane, 1999. Wing Rotation and the Aerodynamic Basis of Insect Flight, *Science*, 284, pp. 1954-1960

T.Maxworthy, 1979. Experiments on the Weis-Fogh mechanism of lift generation by insects in hovering flight. Part. 1 Dynamics of the fling, *J.Fluid Mech.*, 93, part1, pp. 47-63

Robert J. Wood, 2008. The First Takeoff of a Biologically Inspired At-Scale, *IEEE TRANSACTIONS ON ROBOTICS*, 24 (2), pp. 341-1960

De Croon, G.C.H.E., de Clerq, K.M.E., Ruijsink, R., Remes, B., and de Wagter C., 2009. Design, aerodynamics, and vision-based control of the DelFly, *In the International Journal of Micro Air Vehicles*, 1(4), pp. 255-262

Sunada S, Kawachi K, Watanabe I, and Azuma A, 1993. Performance of a Butterfly in Take-off Flight, *Journal of Experimental Biology*, Vol. 183, pp. 249-277

H. Tanaka, K. Hoshino, K. Matsumoto, and I. Shimoyama, 2005. *The 2005 IEEE/RSJ International Conference on Intelligent Robots and Systems (IROS'05)*, pp. 310 – 315, August 2-6, Edmonton, Alberta, Canada

Che-Shu Lin, Chyanbin Hwu and Wen-Bin Young, 2006. The thrust and lift of an ornithopter's membrane wings with simple flapping motion, *Aerospace Science and Technology*, 10, pp. 111-119